Electronic structure studies of six-atom gold clusters

Mohammad A. Omary, Manal A. Rawashdeh-Omary, Charles C. Chusuei, John P. Fackler, Jr., and Paul S. Bagus
Department of Chemistry, P.O. Box 30012, College Station, Texas 77842-3012

(Received 31 January 2001; accepted 30 March 2001)

Combined theoretical and experimental studies of the hexagold phosphine-stabilized complex $[Au_6(PPh_3)_6][BF_4]_2$ (**1**) and of related systems are reported. The goal of these studies is to gain a better understanding of how **1** interacts with the $TiO_2(110)$ substrate to yield finely dispersed supported Au particles that are effective for practical catalytic reactions. The experimental efforts involved the measurement of the visible-ultraviolet (UV) absorption spectra of **1** and $Au(PPh_3)Cl$ in solution. The theoretical efforts involved the determination of the electronic structure of molecular models of **1** based on density functional theory (DFT), Hartree–Fock (HF), and configuration interaction (CI) methods. The CI wave functions and energies were obtained for a range of excited states and were used to simulate the absorption spectra of Au_6 and Au_6^{2+} clusters. The theoretical CI absorption spectra for Au_6 can be correlated with the visible-UV absorption spectra while the theoretical spectra for Au_6^{2+} cannot be correlated with the experiments. This suggests, even though the $[Au_6(PPh_3)_6]$ unit of **1** carries a +2 charge, that the Au_6 portion is essentially neutral. More direct evidence for this distribution of the ionized charge has been obtained from HF and DFT calculations of the double ionization energies of models of **1**. It is found that the energy required to remove two electrons from a bare Au_6 cluster is much larger than that from an Au_6 cluster with phosphine ligands present; this is again consistent with the +2 charge in **1** being delocalized onto the triphenylphosphine ligands. It is possible that this delocalization of positive charge is responsible for facilitating the adhesion of the gold cluster as finely dispersed particles onto the metal oxide support. © *2001 American Institute of Physics.* [DOI: 10.1063/1.1373431]

I. INTRODUCTION

There has been interest in the use of finely dispersed noble metal particles supported on reducible metal–oxide surfaces for applications in heterogeneous catalysis. In particular, highly dispersed, nanosized Au particles supported on TiO_2 have been shown to be especially active in industrially important reactions such as low-temperature CO oxidation[1–4] and the partial oxidation of propylene to propylene oxide.[5,6] Enhanced dispersion of the Au particles increases their activity for these oxidation reactions. Iwasawa and co-workers[7–10] have recently reported the use of the phosphine-stabilized Au complexes $Au(PPh_3)(NO_3)$ and $Au_9(PPh_3)_8(NO_3)_3$ to prepare highly dispersed Au particles on high surface area TiO_2 supports for catalytic applications. Phosphine ligands, when attached to Au clusters of various sizes (e.g., Au_1,Au_4,Au_6,Au_9,Au_{55}, etc.), have been shown to stabilize the clusters, inhibiting them from aggregating,[11] and hence assisting dispersion.

A novel approach has been used recently to deposit a hexagold phosphine-stabilized complex $[Au_6(PPh_3)_6][BF_4]_2$ (**1**) onto a $TiO_2(110)$ single crystal in order to make it amenable for surface probes, which included scanning tunneling microscopy (STM), high resolution electron energy loss spectroscopy, and x-ray photoelectron spectroscopy.[12] Using solution deposition, it was possible to deposit the gold compound as single-unit entities on the substrate, avoiding agglomeration. This was achieved by pretreating the $TiO_2(110)$ crystal with acetone solvent to induce a negative surface charge, thereby assisting the dispersion of the gold clusters. The adsorbed clusters were found to be stable at ambient pressures (~1 atm) for as long as 72 h. Constant current topographic STM images obtained in this experiment showed finely distributed entities of **1** on the $TiO_2(110)$ surface. The STM line profiles showed heights of ~1 nm, corresponding to the expected dimensions of the molecule. However, the reasons underlying the adhesion mechanism leading to the fine dispersion of **1**, i.e., the driving force for surface attachment, are poorly understood. Hence in this followup study, the electronic structure of the hexagold cluster is investigated to gain insight into the nature of its bonding to the metal oxide substrate. In particular, the localization of the charge within the cationic complex is considered.

II. EXPERIMENT

Absorption spectra were carried out for $[Au_6(PPh_3)_6][BF_4]_2$ and $Au(PPh_3)Cl$ using a Hewlett-Packard model HP 8452 ultraviolet (UV)-visible spectrophotometer. The absorption spectra were obtained for solutions of the compounds in freshly distilled reagent grade CH_2Cl_2. The syntheses were carried out by following procedures published elsewhere for $[Au_6(PPh_3)_6][BF_4]_2$[11] and $Au(PPh_3)Cl$.[13]

III. COMPUTATIONAL DETAILS

Density functional theory (DFT),[14] Hartree-Fock (HF),[15] and configuration interaction (CI)[16] theoretical electronic

structure methods were used for calculations of the electronic structure of molecular models of **1**. The models considered were a bare Au_6 cluster and an $Au_6(PH_3)_6$ cluster where the PPh_3 ligands of **1** are represented by PH_3 molecules. Two program systems were used for these calculations; these are the GAUSSIAN 98[17] commercial quantum chemistry program package and the CLIPS (Core Level Ionization Potential System)[18] set of research programs. With both program systems, very similar treatments of the Au atom were made, using a pseudopotential described as an effective core potential (ECP), to represent the 60, $1s^2 2s^2 2p^6 \ldots 4d^{10} 4f^{14}$, core electrons. The parameters for the Au ECP are given by Hay and Wadt;[19] the ECP explicitly includes 19 electrons, from the atomic $5s^2 5p^6 5d^{10} 6s^1$ shells and, hence, it is described as a 19-electron ECP. The ECP[19] incorporates two relativistic effects, mass velocity and Darwin, for the core electrons and, thus, represents the dominant relativistic contributions to the behavior of the 19 outer electrons. The set of $5s$, $5p$, and $3d$ elementary Gaussian type orbital (GTO) basis functions given by Hay and Wadt[19] was used with the calculations performed on both the GAUSSIAN 98 and CLIPS program systems. However, the general, unsegmented contractions to form the contracted GTO, CGTO, basis set for Au were somewhat different. With the GAUSSIAN 98 calculations, the contraction was to $(3s,3p,2d)$ CGTOs and the basis set is double-zeta in the valence region of the Au $5d$, $6s$, and $6p$ shells. With the CLIPS calculations, a somewhat more flexible contraction to $(3s,4p,3d)$ CGTOs was used. The different contractions are not expected to lead to major differences in the quality of the CLIPS and Gaussian calculations.

With GAUSSIAN 98, DFT and HF calculations were performed for the Au_6 and $Au_6(PH_3)_6$ models, treating each as neutral and $+2$ charged systems. The geometries chosen for these molecular models are based on the known crystal structure[20] of **1**. In particular, the geometry of the six Au atoms is that of two tetrahedra with a shared edge (D_{2h} symmetry). For $Au_6(PH_3)_6$, the positions of the Au and P atoms are exactly as in the crystal structure. The H atoms that replace the phenyl groups were placed with the C_{3v} axis of the PH_3 group along the Au–P bond, with P–H=1.25 Å and $\angle$HPH=109.5°.[20(b)] For the bare Au_6 model, the Au positions were kept the same; the PH_3 ligands were simply omitted. In all cases, the calculations were for the closed shell ground states. For the DFT calculations, the Becke three parameter[21] hybrid exchange functional and the Lee–Yang–Parr correlation functional[22] were used. The ECP and basis set for Au were described above; for the all electron treatments of the P and H atoms, Huzinaga/Dunning basis sets of double-zeta quality[23] were used.

With CLIPS, HF and CI calculations were performed for the bare Au_6 and Au_6^{2+} models. An idealized D_{2h} symmetry, taken from Evans and Mingos,[24] with all nearest neighbor Au–Au distances set to 2.70 Å, was used. As with the GAUSSIAN 98 calculations, HF wave functions were determined for the closed shell ground state, which is a ^1A_g state. In addition, excited state CI wave functions and energies were obtained for states that can be excited by absorption of light. The electric dipole allowed transitions are to states that have $^1B_{1u}$, $^1B_{2u}$, and $^1B_{3u}$, symmetries.[25] For these symmetries, single excitation CI wave functions[16] were determined for a large number of states in each symmetry. The configurations included had $N-1$ electrons in the ground state occupied orbitals and 1 electron in a ground state virtual orbital provided that the total symmetry of the configuration was one of the dipole allowed symmetries. For the excitations, it is important to recall that the HF virtual orbitals are not variationally optimized to describe excitations; they are more nearly appropriate for the description of anionic states where an electron is added to Au_6.[16] One of the features of the singles CI is that it corrects this problem by allowing, for any given excited state, a mixture of excitations to be made from the same occupied orbital into several different virtual orbitals. This effective mixing of the virtual orbitals is close to that which would be obtained by using improved virtual orbitals.[16,26] In the singles CI wave function for a particular excited state, excitations from several different occupied orbitals into the same virtual orbital are also mixed. In a similar way, as discussed above, this mixing is equivalent to finding an optimum occupied orbital from which the excitation occurs. These two features effectively use the singles CI to determine optimum, or near optimum orbitals for a one-electron description of an excitation. In addition, the singles CI wave functions also include many body effects that are due to electron correlation. It is possible to distinguish the orbital optimization from the electron correlation effects by examining the natural orbital[16,27] (NO) occupation numbers for each excited state. A measure of the inclusion of true electron correlation effects is the departure of the NO occupation numbers from values of 2, 1, or 0. The departures from these integral NO occupation numbers for the excited states have shown that true electron correlation effects are present to a modest degree in the singles CI wave functions. A particularly important origin for these correlation effects is the mixing of configurations that have excitations from closed shell ground state occupied orbitals to virtual orbitals involving different pairs of symmetries. Let i and j denote indices of occupied orbitals and α and β denote indices of virtual orbitals. Then, for example for an excited state of $^1B_{1u}$ symmetry, the pair of excitations $ia_g \rightarrow \alpha b_{1u}$ and $jb_{1u} \rightarrow \beta a_g$ involve a different pair of symmetries. The mixing of these excitations is an essential electron correlation effect that must be included to give a proper description of the energies and wave functions of the excited states. For wave functions with ^1A_g symmetry, the singles CI would simply give the HF wave function for the closed shell ground state; hence, these CI calculations were not performed and the HF wave function was used for the ground state. In order to reduce the size of the CI calculation, the numbers of the occupied and virtual orbitals used in the CI was reduced from the full spaces of these orbitals. In each symmetry, a few of the lowest lying occupied orbitals and a few of the highest lying virtual orbitals were excluded from the CI calculation. This exclusion is not expected to change the results in any significant way from that which would be obtained with the use of the fully occupied and virtual spaces.

Dipole transition matrix elements (MEs) were computed between the ground state HF wave function and the excited state CI wave functions; these matrix elements were used to

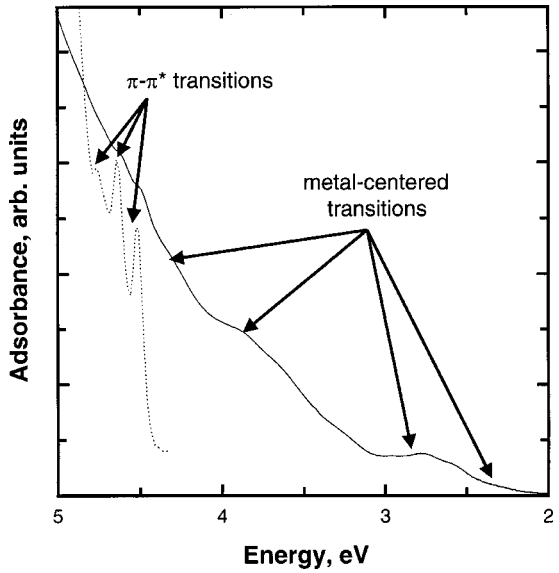

FIG. 1. UV-visible absorption spectra of **1** (solid line) and $Au(PPh_3)Cl$ (dashed line) in CH_2Cl_2 solutions at ambient temperature.

generate a theoretical electronic excitation spectrum for the Au_6 cluster. The MEs were taken for the dipole length operator,[28] **r** or *x*, *y*, and *z*. With the choice made for the axes of the coordinate system used for the Au_6 cluster, only the operator *x* has nonzero MEs for excitations from the ^1A_g to $^1B_{2u}$ states, the operator *y* has nonzero MEs for ^1A_g to $^1B_{3u}$, and the operator *z* has nonzero ME for ^1A_g to $^1B_{1u}$. For each of the excited state symmetries, MEs were computed for excited states with energies up to ~4.2 eV above the first excited state in that symmetry. Overall, MEs for excitations up to ~8 eV above the ground state were considered. For comparison with the experimental UV-visible spectrum of **1** where the exciting radiation is not polarized and where the excited molecules are not oriented in space, it is appropriate to average the transition probabilities over the *x*, *y*, and *z* directions. We will describe the results for different polarizations of the transition ME as a way to distinguish, at least partly, the different excited states of Au_6. The dipole length matrix element between the ground state (state 1) and an excited state (state *j*) is given by the vector $\mathbf{T}_{1j}$:

$$\mathbf{T}_{1j}=\langle\Psi_1|\mathbf{r}|\Psi_j\rangle, \tag{1}$$

where, as noted above, only one component of $\mathbf{T}_{1j}$ is nonzero for any given excited state *j*. In terms of the ME $\mathbf{T}_{1j}$, the intensity of absorbed radiation I_{1j} is given by[28]

$$I_{1j}\propto(\Delta E_j)^3|\mathbf{T}_{1j}|^2, \tag{2}$$

where $\Delta E_j=E_j-E_1$ is the calculated excitation energy to the *j*th excited state. Below, we present the theoretical absorption spectra in the form of histograms or bar charts.

IV. RESULTS AND DISCUSSION

A. Experimental spectra

Figure 1 shows the absorption spectrum of a 8.3×10^{-5} M solution of **1** in CH_2Cl_2. The spectrum shows continuous absorption at energies >2 eV, with pronounced features near 2.3, 2.7, 3.3, 4.0, 4.3, and above 4.5 eV. The profile of the absorption spectrum is independent of concentration, suggesting that the hexanuclear cluster unit in **1** is the major absorbing species with no further aggregation in dichloromethane (solutions with concentration near saturation gave essentially the same absorption profile shown in Fig. 1). In order to gain insight into the assignment of the absorption peaks, an absorption spectrum of a CH_2Cl_2 solution of $Au(PPh_3)Cl$ is also included for comparison. This solution exhibits well-resolved absorption peaks between 4.6 and 5.0 eV, characteristic of $\pi-\pi^*$ transitions for the triphenylphosphine ligand.[29] These peaks are not expected to be affected by the clustering of the gold–triphenylphosphine adduct. Indeed, the same features are observed in the spectrum of **1**. We therefore assign the absorption peaks with energies >4.5 eV in the spectrum of **1** to intraligand $\pi-\pi^*$ transitions. Clustering of Au atoms leads to a reduction in the HOMO–LUMO gap relative to monomer units. This is evident even to the naked eye, as **1** is deeply colored (dark red) while $Au(PPh_3)Cl$ is colorless [typical of mononuclear complexes of Au(I) and Au(0) with phosphine ligands]. Therefore, the low energy features of the absorption spectrum of **1** are due to metal-centered transitions of the Au_6 cluster. Consequently, in the models used to calculate the absorption spectrum of **1**, it is reasonable to use ''bare'' Au_6 clusters without ligands.

B. Calculated spectra

The theoretical transition energies and relative absorption intensities, see Eq. (2), were calculated with the HF wave functions for the ^1A_g ground state and CI wave functions for the excited states of the Au_6^0 and Au_6^{2+} cluster. First, we describe the results for the neutral Au_6^0 cluster. The excitation energies (in eV) and the relative absorption intensities (in parentheses) to the first excited state for the allowed $^1B_{2u}$ (or *x*), $^1B_{3u}$ (or *y*), and $^1B_{1u}$ (or *z*) symmetries, respectively, are: 2.24 (55.0), 3.87 (151.5), and 1.89 (8.0). Of these transitions, the $^1A_g\rightarrow{}^1B_{3u}$ is the most intense. Figure 2 shows spectral intensities from each of the three electric–dipole allowed transitions for the neutral Au_6^0 center. The individual CI spectral transitions were combined in order to obtain a composite spectrum of the bare Au_6^0 cluster [Fig. 3(a)]. For the charged Au_6^{2+} cluster, the theoretical CI electronic excitation energies and absorption intensities are very different from those for the neutral Au_6^0 cluster. The excitation energies (in eV) and the relative absorption intensities (in parentheses) to the first excited $^1B_{2u}$, $^1B_{3u}$, and $^1B_{1u}$ states, respectively, are: 4.07 (33.8), 4.73 (15.8), and 4.39 eV (141.8). These lowest excited states are at considerably higher energies than those for the neutral Au_6^0 cluster and the transition intensities have a very different pattern. The strongest absorption peaks appear at energies of 5.3, 6.8, and 7.3 eV for excitations from the ^1A_g ground state to the $^1B_{2u}$, $^1B_{3u}$, and $^1B_{1u}$ excited states, respectively. The contributions of the three manifolds of symmetry allowed transitions were combined to obtain the composite theoretical optical spectrum of Au_6^{2+} given in Fig. 3(b).

While comparing the calculated spectra in Fig. 3 with

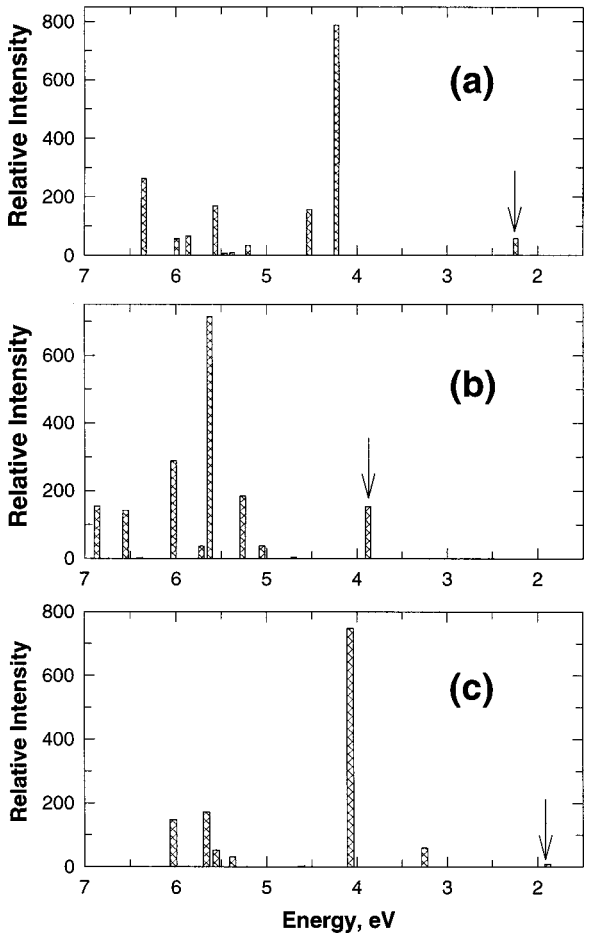

FIG. 2. CI calculated spectra of Au_6^0. Intensities are shown for the: (a) $A_g \rightarrow {}^1B_{2u}$, (b) $A_g \rightarrow {}^1B_{3u}$, and (c) $A_g \rightarrow {}^1B_{1u}$ transitions. The arrows denote the first root intensities obtained from diagonalization of the Hamiltonian matrices.

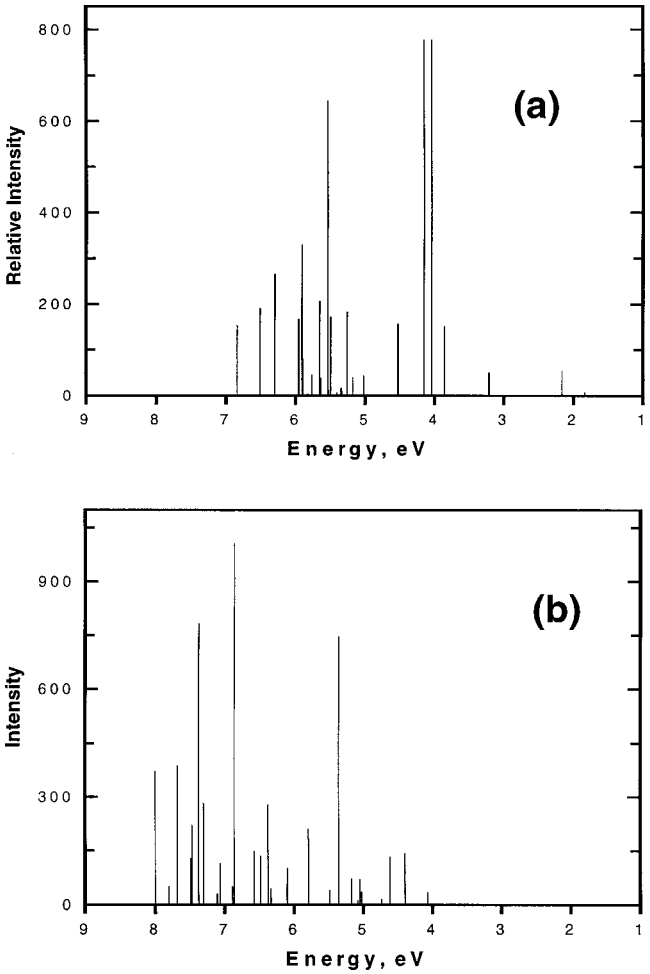

FIG. 3. Composite CI spectra for: (a) bare Au_6^0 cluster; (b) bare Au_6^{2+} cluster.

the absorption spectrum of **1** in Fig. 1, it is important to note that inhomogeneous broadening due to solvent interactions as well as instrumental limitations lead to the low resolution of the absorption peaks, compared with the sharp lines obtained from the calculation using the CI method. The theoretical CI absorption spectrum for the neutral Au_6^0 cluster shows reasonable agreement with the experimental absorption spectrum (Fig. 1). The aforementioned features in the experimental absorption spectrum (between 2.0 and 4.5 eV) are clearly evident in the calculated spectrum for Au_6^0 with qualitatively similar energies and relative intensities. Metal-centered transitions at the high-energy region ($>$4.5 eV) are also predicted by the CI calculations for Au_6^0. However, these transitions are masked by the intense $\pi \rightarrow \pi^*$ intraligand transitions as well as the solvent cutoff in the absorption spectrum. In contrast to Au_6^0, the calculated spectrum for the cationic Au_6^{2+} cluster is vastly different from the experimental absorption spectrum of **1**. The calculated spectrum for the Au_6^{2+} cluster shows absorptions only at energies $>$4 eV with the strongest peaks at $>$5 eV, thus not accounting for the strong absorptions at much lower energies in the experimental spectrum of **1**.

The assignment of the low-energy features in the absorption spectrum of **1** to metal-centered transitions is also supported by the charge distributions of the high-lying occupied and low-lying virtual unoccupied orbitals of the phosphine-containing model cluster $[Au_6(PH_3)_6]^{2+}$. The contour plots of the DFT Kohn–Sham HOMO and LUMO for this molecular model given in Fig. 4 show that the electron density of these orbitals is to a large degree localized on the Au atoms. This is a strong indication that the lowest energy electronic excitation, from HOMO to LUMO, is a metal centered transition. We have also examined the coefficients in the molecular orbital (MO) expansions in terms of the basis functions for both the HF and DFT frontier orbitals. For the HOMO and LUMO, the large MO coefficients are for basis functions centered on the Au atoms while, in general, the basis functions centered on the P and H atoms have small MO coefficients. This is also true for several other frontier orbitals so that still other low-lying excitations in $[Au_6(PH_3)_6]^{2+}$ should be dominated by metal-centered transitions as well.

C. Ionization energies

Based on the results described above, we suggest that the charge removed from the hexagold phosphine complex in **1** to form the dictation is taken dominantly from the PPh_3 ligands. In other words, the $+2$ charge in **1** is delocalized

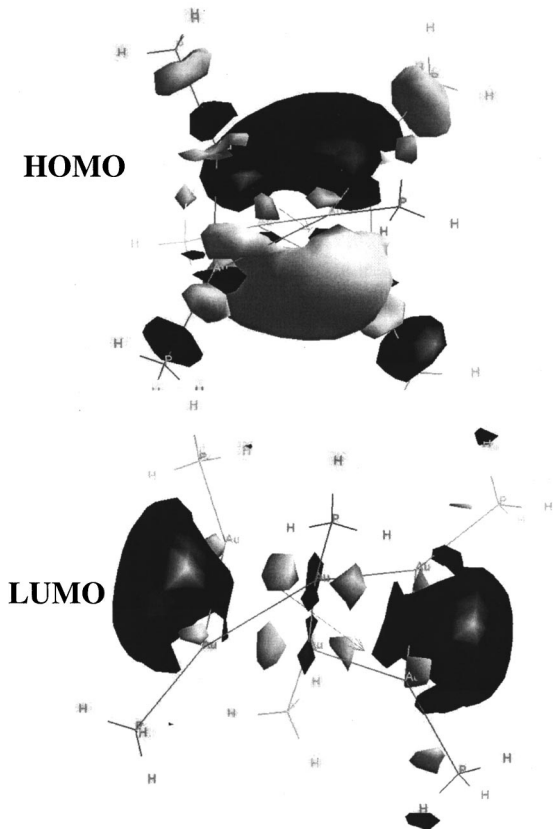

FIG. 4. Contour plots of the HOMO and the LUMO for the $[Au_6(PH_3)_6]^{2+}$ model used in DFT calculations.

onto the triphenylphosphine ligands. Another property that can help identify the origin of the ionized charge in **1** is the ionization energy or ionization potential (IP) from the neutral to the +2 ion cluster. We denote these IPs to the +2 ion as IP^{+2}; the theoretical values of the IPs are obtained by taking the differences of the calculated total energies as $IP^{+2} = E(X^{+2}) - E(X^0)$, where X is the system that is being ionized. Specifically, our concern is to compare the values of IP^{+2} for the bare Au_6 cluster and for the cluster model which includes phosphine ligands, $Au_6(PH_3)_6$. Large differences between the IPs for these cluster models might suggest that the origin of the ionized charge is different in the two clusters. On the other hand, similar values of the IPs for the two clusters would indicate that the charge to form the +2 ion comes dominantly from the Au atoms. The values of IP^{+2} obtained from the GAUSSIAN 98 HF and DFT calculations are given in Table I.

The data in Table I clearly show that the energy required to remove two electrons from a bare Au_6 cluster is much higher than the corresponding ionization energy for the ligand-containing clusters $Au_6(PH_3)_6$. The HF and DFT methods give rise to higher ionization energy for the bare Au_6 cluster by 8.3 and 9.8 eV, respectively, i.e., more than twice the energy required for the ionization of $Au_6(PH_3)_6$. The large IP^{+2} for the bare Au_6 cluster can be understood in terms of the limiting cases of a single Au atom and bulk Au metal. For an Au atom,[30] the first IP is 9.2 eV and the second IP is 20.5 eV giving $IP^{+2} = 29.7$ eV. For Au metal, the work function[31] ϕ is 5.8 eV and the double IP is simply two times ϕ or $IP^{+2} = 11.6$ eV. It is reasonable, given its small size, that the IPs of the Au_6 cluster should be significantly larger than those for bulk metal Au. Thus, the calculated values of $IP^{+2} \approx 15$ eV (see Table I) are hardly surprising. The difference of the DFT and HF values in Table I for the IP^{+2} of Au_6 might appear large at first sight. We have examined the DFT and HF values of the first and second IPs for an isolated Au atom and have found that the differences of the IP^{+2} for the cluster are about what would be expected for the different errors of the two approximations. For the HF method, the IPs are normally expected to be smaller than the exact values,[32] while the IPs may be overestimated with the DFT method. However, since the DFT treatment includes correlation effects, the error for the DFT IPs should normally be significantly smaller than the error for the HF IPs. For a bare Au atom, GAUSSIAN 98 calculations using HF and DFT methods gave IP^{+2} values of 26.9 and 30.4 eV, respectively, representing respective deviations of −2.8 and +0.7 eV from the experimental value of 29.7 eV.

The much lower double ionization energy for the phosphine containing $Au_6(PH_3)_6$ cluster is consistent with the charge being removed from the PH_3 groups. This is because the large polarizability of Au_6 will allow the Au charge to polarize in response to the presence of $(PH_3)^+$ ions and hence to lower the phosphine IP. The presence of phenyl rings in **1**, which were not accounted for in the GAUSSIAN 98 calculations,[33] is expected to lead to IP's even lower than those calculated when the ligands are PH_3. First, the large size of the phenyl rings may allow a strong delocalization of the positive charge in an ionized PPh_3 unit thus lowering its IP. Second, PPh_3 may act as a π acceptor, further lowering its IP in the $Au_6(PPh_3)_6$ cluster. Recent reports in the literature provide additional support for these conclusions. Dougherty[34] has reported that various aromatic compounds, including benzene, can interact with various cations giving rise to cation-π interactions. Fackler *et al.*[35] have recently reported similar type of interactions between some trinuclear gold(I) centers and various cations and neutral acid complexes.

The charge distribution results presented here have important implications for the action of **1** on metal oxide surfaces for the preparation of practical catalyst systems. In fact, **1** has recently been employed successfully in the preparation of a Au/TiO_2 high surface area catalyst, which showed high activity for CO oxidation with a very minimal decrease in turnover frequency after subsequent regeneration treatments.[36] The delocalization of the +2 charge onto the triphenylphosphine ligands could act to enhance the electrostatic interactions with a negatively charged $TiO_2(110)$ metal

TABLE I. The double ionization potentials, IP^{+2} in eV, for the Au_6 and $Au_6(PH_3)_6$ cluster models obtained from HF and DFT calculations. The IP^{+2} values are calculated as the differences in the total energies between the neutral and +2 charged systems.

Model	IP^{+2}/HF	IP^{+2}/DFT
$Au_6(PH_3)_6$	5.88	8.28
Au_6	14.20	17.94

oxide support by bringing the positive charge closer to the surface. Furthermore, the agglomeration of **1** is inhibited due to repulsive forces between the charged cluster units, in agreement with the optical results, which show the invariance of the absorption spectra with concentration (*vide supra*). Charge delocalization onto the ligands, using PH_3 as a model for PPh_3, is further supported by the electrostatic potentials calculated for aromatic rings.[34,35(b)] At the center of the rings, these potentials are negative while at the periphery of the rings they are positive. The negative electrostatic potentials at the centers of the phenyl rings in a PPH_3 unit in **1** could help to reduce the IP of this unit. This is further evidence to indicate that the IP of a $Au_6(PPh_3)_6$ cluster should be smaller than the IP of the model system of $Au_6(PH_3)_6$ that we studied. On the other hand, the positive electrostatic potentials in the peripheral regions of the phenyl rings enhance the repulsion between adjacent cluster units. The charge effects discussed herein therefore help to explain the high surface dispersion of **1** on the $TiO_2(110)$ surface.

V. CONCLUSIONS

The electronic absorption spectrum of **1** has been compared with theoretical spectra for both neutral and charged bare Au clusters, Au_6 and Au_6^{2+}. The theoretical absorption spectra are based on CI wave functions for a large number of excited states, up to ~8 eV above the ground state, with the transition matrix elements calculated between the HF ground state and these CI excited state wave functions. The observed absorption spectrum shows a better resemblance to the theoretical spectrum for Au_6^0 than to that for Au_6^{2+}, suggesting that the Au_6 metal cluster center is virtually neutral. This was confirmed by HF and DFT calculations, which show much lower ionization energies for $Au_6(PH_3)_6$ with phosphine ligands versus the Au_6 cluster without ligands. The experimental and theoretical results herein thus provide evidence for the delocalization of the +2 charge in **1** onto the triphenylphosphine ligands. In addition to stabilizing the hexagold center and inhibiting Au atom agglomeration, the charge delocalization gives rise to high dispersion of the clusters onto metal–oxide supports via electrostatic interactions, which include: (1) attractive forces leading to the bonding of the complex to the electron-rich $TiO_2(110)$ surface and (2) repulsive forces between neighboring clusters, thus hindering aggregation. These effects would likely increase the dispersion of the Au nanostructure on the metal–oxide support. Recent experimental results[36] indicate that dispersed Au clusters have, after removal of the phosphine ligands, a high catalytic activity for CO oxidation.

ACKNOWLEDGMENTS

Most importantly, we wish to express our heartfelt appreciation and gratitude for the stimulation and encouragement that Dr. D. Wayne Goodman, Texas A&M University, provided throughout the progress of our work. We acknowledge the support of this work by the Department of Energy, Office of Basic Energy Sciences, Division of Chemical Sciences, the Robert A. Welch Foundation and the Dow Chemical Company. We are pleased to acknowledge the computer support provided by the National Center for Supercomputing Applications at Urbana-Champaign, Illinois, and the Laboratory for Molecular Simulations at Texas A&M University. C.C.C. gratefully acknowledges the Associated Western Universities, Inc. and the Pacific Northwest National Laboratory operated by Batelle Memorial for support. We also thank Dr. Paul R. Sharp, the University of Missouri at Columbia, for providing the gold cluster for use in our studies and for stimulating discussions.

[1] M. Haruta, S. Tsubota, T. Kobayashi, H. Kageyama, M. J. Genet, and B. Delmon, J. Catal. **144**, 175 (1993).
[2] M. Haruta, Catal. Today **36**, 153 (1997).
[3] J.-D. Grunwaldt and A. Baiker, J. Phys. Chem. B **103**, 1002 (1999).
[4] J.-D. Grunwaldt, C. Kiener, C. Wögerbauer, and A. Baiker, J. Catal. **181**, 223 (1999).
[5] T. Hayashi, K. Tanaka, and M. Haruta, J. Catal. **178**, 566 (1998).
[6] M. Haruta, in *3rd World Congress on Oxidation Catalysis*, edited by R. K. Grasselli, S. T. Oyama, A. M. Gaffney, and J. E. Lyons (Elsevier Science, Amsterdam, 1997), Vol. 109, pp. 123–134.
[7] Y. Yuan, K. Asakura, H. Wan, K. Tsai, and Y. Iwasawa, Catal. Lett. **42**, 15 (1996).
[8] Y. Yuan, K. Asakura, H. Wan, K. Tsai, and Y. Iwasawa, Chem. Lett. **1996**, 755.
[9] Y. Yuan, A. P. Kozlova, K. Asakura, H. Wan, K. Tsai, and Y. Iwasawa, J. Catal. **170**, 191 (1997).
[10] Y. Yuan, K. Asakura, A. P. Kozlova, H. Wan, K. Tsai, and Y. Iwasawa, Catal. Today **44**, 333 (1998).
[11] (a) V. Ramamoorthy, Z. Y. Wu, Y. Yi, and P. R. Sharp, J. Am. Chem. Soc. **114**, 1526 (1992); (b) P. J. Dyson and D. M. P. Mingos, in *Gold: Progress in Chemistry, Biochemistry and Technology*, edited by H. Schmidbaur (Wiley, New York, 1999), pp. 511–556; (c) B. W. Flint, Y. Yang, and P. R. Sharp, Inorg. Chem. **39**, 602 (2000).
[12] C. C. Chusuei, X. Lai, K. A. Davis, E. K. Bowers, J. P. Fackler, Jr., and D. W. Goodman, Langmuir (in press).
[13] C. A. McAuliffe, R. V. Parish, and P. D. Randall, J. Chem. Soc. Dalton Trans. **1979**, 1730 (1979).
[14] R. G. Parr and W. Yang, *Density-Functional Theory of Atoms and Molecules* (Oxford University Press, Oxford, 1989).
[15] (a) C. C. J. Roothan, Rev. Mod. Phys. **23**, 69 (1951); (b) C. C. J. Roothaan, *ibid.* **32**, 179 (1960); (c) J. A. Pople and R. K. Nesbet, J. Chem. Phys. **22**, 571 (1954); (d) R. McWeeny and G. Dierksen, *ibid.* **49**, 4852 (1968).
[16] (a) J. B. Foresman, M. Head-Gordon, J. A. Pople, and M. J. Frisch, J. Phys. Chem. **96**, 135 (1992); (b) See, for example, H. F. Schaefer III, *The Electronic Structure of Atoms and Molecules* (Addison-Wesley, Reading, MA, 1972) for a general description of various theoretical methods and for further references.
[17] M. J. Frisch *et al.*, GAUSSIAN 98, Revision A. 6 (Gaussian, Inc., Pittsburgh PA, 1998).
[18] CLIPS is a quantum chemistry program system for the computation of ab initio SCF and correlated, CI, wave functions for polyatomic systems. It has been developed based on the publicly available programs in the ALCHEMY package from the IBM San Jose Research Laboratory.
[19] P. J. Hay and W. R. Wadt, J. Chem. Phys. **82**, 270 (1985).
[20] (a) C. E. Briant, K. P. Hall, D. M. P. Mingos, and A. C. Wheeler, J. Chem. Soc. Dalton Trans. **1986**, 687. (b) The crystal structure of **1** was downloaded from the Cambridge Crystal Structure Database. All graphical manipulations to produce the models and GAUSSIAN 98 input files were done using Cerius^2 (Release 4.0, Molecular Simulations Inc., 1999). The force field in Cerius^2 was used to optimize the positions of the H atoms in the PH_3 units.
[21] A. D. Becke, J. Chem. Phys. **98**, 5648 (1993).
[22] (a) C. Lee, W. Yang, and R. G. Parr, Phys. Rev. B **37**, 785 (1988); (b) B. Miehlich, A. Savin, H. Stoll, and H. Preuss, Chem. Phys. Lett. **157**, 200 (1989).
[23] T. H. Dunning, Jr. and P. J. Hay, in *Modern Theoretical Chemistry*, edited by H. F. Schaefer III (Plenum, New York, 1976), Vol. 3, p. 1.
[24] D. G. Evans and D. M. P. Mingos, J. Organomet. Chem. **232**, 171 (1982).
[25] For properties of the D_{2h} point group, see, for example, F. A. Cotton, *Chemical Applications of Group Theory* (Wiley, New York, 1971).

[26] (a) U. Wahlgren, Mol. Phys. **33**, 1109 (1977); (b) W. J. Hunt and W. A. Goddard, Chem. Phys. Lett. **3**, 414 (1969).
[27] See, for example, B. O. Roos, P. R. Taylor, and P. E. M. Seigbahn, Chem. Phys. **48**, 157 (1980).
[28] H. A. Bethe and E. E. Salpeter, *Quantum Mechanics of One-and Two-Electron Atoms* (Academic, New York, 1957).
[29] L. J. Larson, E. M. McCauley, B. Weissbart, and D. S. Tinti, J. Phys. Chem. **99**, 7218 (1995).
[30] C. E. Moore, *Atomic Energy Levels*, Natl. Bur. Stand. No. 467 (U.S. GPO, Washington, D.C., 1952).
[31] *CRC Handbook of Chemistry and Physics*, 76th ed. (CRC Press, Boca Raton, FL, 1995).
[32] P. S. Bagus, Phys. Rev. **139**, A619 (1965).
[33] If calculations similar to those described here were performed for the $Au_6(PPh_3)_6$ system, the basis set would have to contain more than 1300 contracted Gaussian type orbital basis functions. Thus, the requirements for HF, CI, and DFT calculations, in terms of computer time and memory, would be extremely large.
[34] D. A. Dougherty, Science **271**, 163 (1996), and references therein.
[35] (a) A. Burini, R. Bravi, J. P. Fackler, Jr., R. Galassi, T. A. Grant, M. A. Omary, B. R. Pietroni, and R. J. Staples, Inorg. Chem. **39**, 3158 (2000); (b) A. Burini, J. P. Fackler Jr., R. Galassi, T. A. Grant, M. A. Omary, M. A. Rawashdeh-Omary, B. R. Pietroni, and R. J. Staples, J. Am. Chem. Soc. **122**, 11264 (2000).
[36] T. V. Choudhary, C. Sivadinarayana, C. C. Chusuei, and D. W. Goodman (unpublished).